On Soil Deformation and Stress Redistribution Around Pressed-in and Vibrated Displacement Pile Tips

J. Vogelsang, G. Huber and Th. Triantafyllidis

Abstract The experimental study compares soil displacement trajectories around model pile tips obtained from Digital Image Correlation (DIC) for different penetration modes. Monotonic and cyclic quasi-static penetration under plane strain-resembling conditions in dry sand and vibratory model pile penetration in saturated sand are investigated. The comparison results agree well although the penetration mode and the degree of saturation differ considerably. In the experiments, the soil below the pile tip is first pushed downwards as the pile approaches and is then moved more and more sidewards. A slight uplift of the grains is observed when the pile tip has passed. Subsequently, a clear trend of the soil adjacent to the pile shaft to move towards the pile is measured in the case of quasistatic cyclic and vibratory penetration. This trend is considered to be an indicator for "*friction fatigue*", the degradation of shaft friction at a certain depth as the pile penetrates further. A discussion on the comparability with numerical results and on the influence of disturbing boundary effects concludes this contribution.

Keywords Pile penetration · Vibratory pile driving · Friction fatigue

1 Introduction

The application of Digital Image Correlation (DIC) to geotechnical model tests on pile penetration has been an important improvement for understanding related effects. Substantial efforts have been made on the evaluation of soil displacements

J. Vogelsang (✉) · G. Huber · Th. Triantafyllidis
Institute of Soil Mechanics and Rock Mechanics, Karlsruhe Institute of Technology, Karlsruhe, Germany

Th. Triantafyllidis
e-mail: triantafyllidis@kit.edu

Th. Triantafyllidis (ed.), *Holistic Simulation of Geotechnical Installation Processes*, Lecture Notes in Applied and Computational Mechanics 77,
DOI 10.1007/978-3-319-18170-7_3

and deformation around pile tips with small diameter, e.g. [15]. However, most work concentrates on small, non-instrumented model piles penetrating into dry material in monotonic penetration mode. The measurement of stresses acting on the pile is usually performed in closed test devices (strong boxes or calibration chambers) without evaluation of soil deformation [3, 4, 16]. Important phenomena, like e.g. *friction fatigue*, were measured in such tests. These effects were also investigated via DIC in tests with non-instrumented piles by consideration of characteristics of displacement and strain paths [15]. The attribution of these optical observations to stress measurements in the same test is still a challenging task.

The aim of this paper is to contribute to this research work and to provide reliable experimental data for the validation of Finite Element (FE)-simulation techniques. Therefore, 1g-model tests were performed to investigate the soil mechanical effects around pile tips during pressed-in and vibrated-in penetration modes in coarse grained material. A cohesionless medium quartz sand was used in all tests. Two test devices were used: a large scale test device with 2D-resembling conditions for pressed-in sheet-like piles and a half cylinder-shaped device for rectangular vibro-driven piles. Both devices allow the evaluation of soil displacements and deformations around the pile tip via DIC. In this contribution displacement trajectories and principal strains (resp. strain directions) will be analysed. Major subjects of this study were penetration mode and pile tip geometry. Quasi-static monotonic and cyclic penetration were investigated using the large scale test device. Vibratory penetration was performed in the second test device. Both will be quantitatively compared in terms of displacement and strain paths. Remarks on the transferability of the test results on real displacement piles and the limitations of model testing will be made. A comparison of test results and effects of pile driving observed in FE simulations will conclude this contribution.

2 Experimental Methods and Setup

The interface test device with possible test configurations is presented in detail e.g. in [8, 12, 16]. The setup used in this study is illustrated schematically in Fig. 1. The so-called 2D-pile is a wall structure with 0.5 m width placed between two glass observation windows. This 2D-pile is divided into four instrumented segments in order to evaluate the force distribution on the structure. In the second segment, the "pile tip" is located. Thus, the lowest segment and the lower part of the second segment represent a kind of pre-pile. Segments three and four represent the pile shaft. This assembly resembles the zipper-technique, that is often used in FE simulations of pile penetration. The glass windows have relatively smooth surfaces and are reinforced horizontally. This experimental setup tries to achieve plane-strain conditions (which is actually not completely successfull, see [13] and Sect. 6.2). The 2D-pile is penetrated into the sand using an hydraulic actuator mounted on top of the test device. This actuator moves a connection rod that is coupled individually to each wall segment. The 2D-pile is 15 mm wide (b_{pile} = 30 mm) and has a tip inclination of 30°.

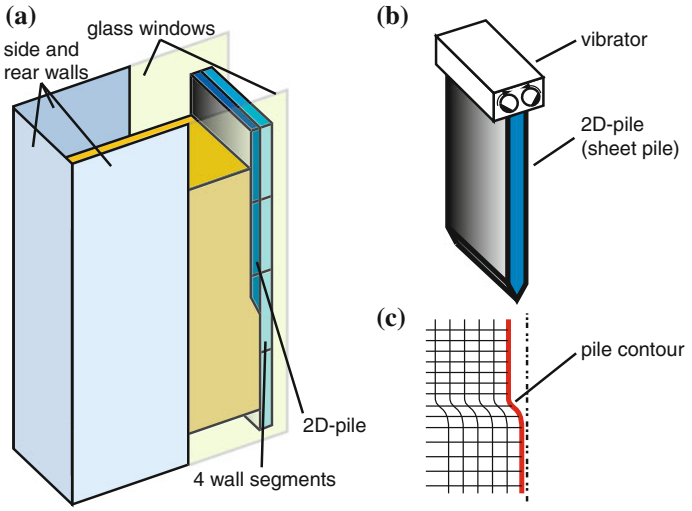

Fig. 1 **a** Schematic interface test device, **b** sketch of a 2D-pile (*sheet pile*) and **c** corresponding FE-mesh with pre-pile

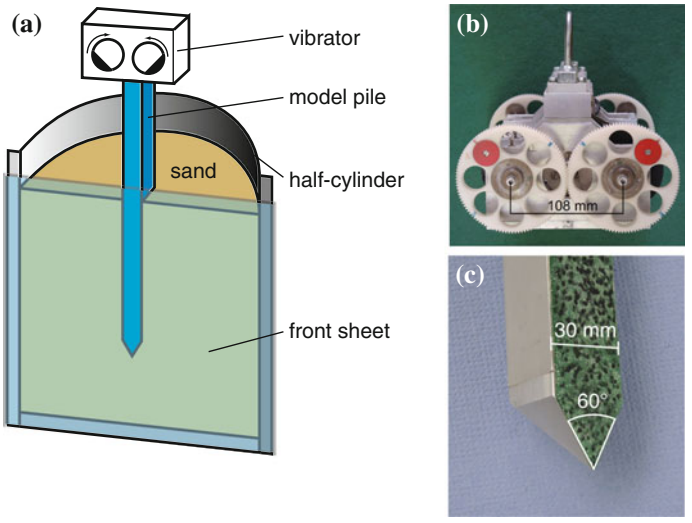

Fig. 2 **a** Test device for vibro penetration, **b** vibrator and **c** detail pile tip

In the half-cylinder test device, model tests with water saturated sand are possible. Model piles with small equivalent diameter can be penetrated into the sand by vibro-driving. They slide along the acrylic glas front sheet, so that the pile tip and one face are visible throughout the whole test. A schematic illustration of this test device is shown in Fig. 2a. The model piles are driven by a small vibrator, Fig. 2b.

The model pile shaft is an aluminium tube with rectangular cross sections of 30×30 mm and 2 mm wall thickness. The tip geometry was matched to the 2D-pile tip in order to provide comparable geometric effects. It has a pyramidal shape with the same width as the shaft and a cone angle of 60° (same angle as 2D-pile tip) resp. 45° (back), see Fig. 2c. The front face of the pyramid is vertical and is in contact with the front sheet (observation window). A layer of felt is bonded to the surface in contact with the acrylic glas front in order to ensure low friction between the pile and the window.

2.1 Instrumentation

Substantial force and stress measurements are possible in the case of the large scale test device. They include measurement of horizontal and vertical support forces on the wall segments. A detailed discussion on the evaluation of tip resistance and earth pressure distribution is provided in [12]. The displacement is measured separately for each wall segment.

In the half-cylinder, only pile head force and pile displacement are measured. The load cell is placed between vibrator and pile. The displacement is measured with a rope pulley transducer.

2.2 Evaluation of Soil Deformation

Both test device have glas resp. acrylic glas observation windows allowing the evaluation of soil deformations during the tests. In the interface test device, the front and rear side walls in vicinity to the wall segments are glass windows. The half-cylinder has a acrylic glas sheet in the symmetry plane. In both cases, the observation windows are assumed to behave similarly to symmetry planes.

2.2.1 Digital Photography and Post-processing

Three digital cameras are used in interval mode for the observation of quasi-static tests. The dynamic model pile penetration is documented using a high frequency video camera. Information on cameras and picture recording are given in Table 1.

Representative sections of the test are subsequently extracted from the image sequences. If necessary, the image sequences are post-processed. Post-processing includes fine rotation with respect to known vertical or horizontal axes. Cropping the regions of interest is done inside the DIC software JPIV [10]. Figure 3 shows image material taken from two test using both test devices. It can be seen that a random pattern is painted on the felt in order to provide a sufficient contrast for DIC.

Table 1 Camera information

	Pressed-in piles	Vibro-driven piles
Camera	Nikon coolpix P7700	Basler CMOSIS ace acA2000-340km
File type	xxx.jpg	xxx.seq
Interval (s)	30	0.007
Images per min	2	8400
Size (Pixel)	2816 × 2112	2040 × 1088
Scale (Pixel/mm)	≈15	≈10
Scale (Pixel/d_{50} (mm))	≈8	≈5
Color depth (bit)	24	8

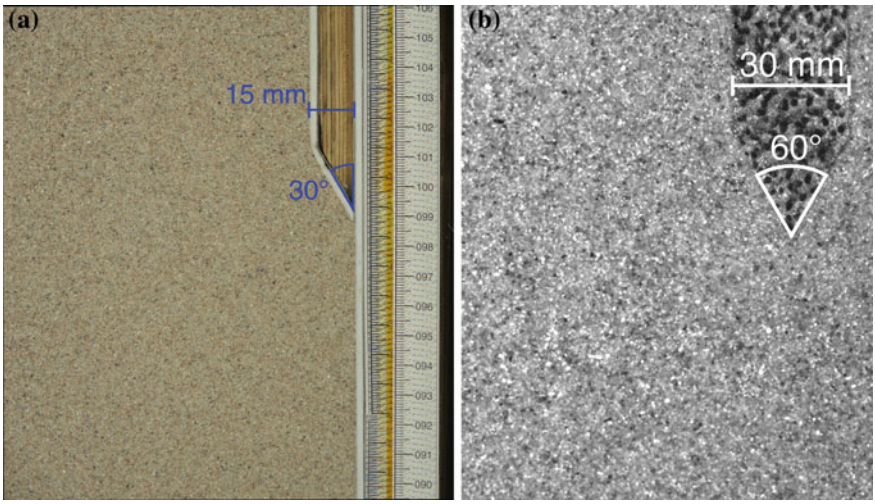

Fig. 3 Image material from **a** 2D-pile penetration and **b** 3D-vibrodriven pile penetration

A correct evaluation of the pile displacement is important, because it is the only part of the image where the quality of the evaluation can be proved.

2.2.2 Digital Image Correlation

JPIV [10], a freeware code for Particle Image Velocimetry, is used for the evaluation of the displacement field between two subsequent images. Summation of the displacements and strain calculation is done afterwards. The evaluation procedure is described in [8, 16].

2.3 Test Material, Sample Preparation, and Uniformity Control

A medium silica (quartz) sand is used in the experiments. Some important granular properties are given in [11, 14]. The sand is installed in the test device by using a sand rainer system (described in detail in [8, 16]). Before the test, the uniformity of the soil sample is controlled by CPTs. The set-up, evaluation procedure and first results are discussed in [13].

2.3.1 Dry Conditions

Dry samples for the large scale interface test device are obtained by air pluviation of dry material. Details on the pluviation system and methods can be found in [8, 16]. Note that the initial stress state before the test is influenced by silo effects. An investigation of these effects is provided in [13].

2.3.2 Saturated Conditions

Saturated samples in the half-cylindrical test device are obtained by pluviation of dry material into water. This procedure results in relative densities of about 40 %. Higher densities can be achieved by excitation of the test device with slight hammer blows against the side walls. The densification was stopped when a relative density of about 70 % has been reached. This method is considered to provide high degrees of saturation [17]. However, subsequent densification of the soil body is not applicable in all test devices. In addition to this, the uniformity of the sample has to be ensured.

3 Nomenclature, Coordinates, and Sign Conventions

A schematic illustration of the model pile embedded in sand is shown in Fig. 4 with the relevant geometries and the chosen coordinate system. The pile diameter in the view plane is denoted b_{pile}. The width of the 2D-pile corresponds to $b_{\text{pile}}/2$. A local coordinate system is defined relative to the initial pile position. The origin is located in the symmetry axis/plane of the pile on the vertical level of the pile shoulder. Coordinates downwards and to the left are defined negative. In the deformed configuration, the current vertical distance between an arbitrary sand element and the pile shoulder is named Δy (also negative towards bottom and left), Fig. 4c. A sand element below the pile tip has thus a negative Δy. According to [15], this coordinate will be presented in a normalized form: $2\Delta y/b_{\text{pile}}$. For selected points on the displacement trajectory, the deformed element shape will be plotted in the directions of principal strain. This configuration is schematically illustrated in Fig. 4d.

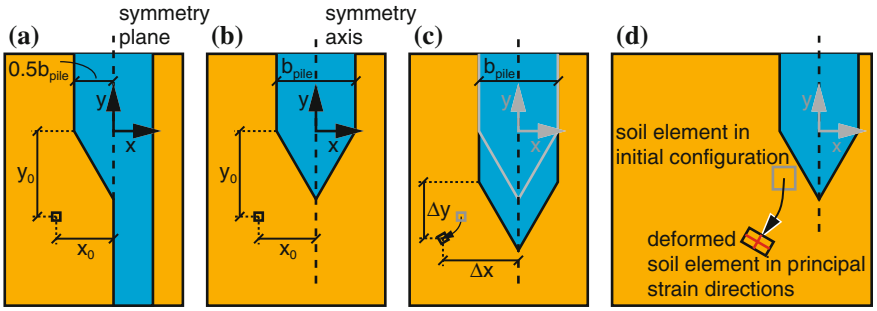

Fig. 4 Coordinate system relative to pile tip: **a** 2D-pile, **b** 3D-pile, **c** coordinates relative to current pile position and illustration of displacement trajectory and **d** element shape in deformed configuration in directions of principal strain

Table 2 Information concerning the compared tests

Test	Dim.	Tip shape	Penetration mode	I_D (%)	S_R (%)	h_{sand} (m)	$\sigma_{y,0}$ (kN/m^2)
V18-1	2D	2D-30°	Monotonic	69	0	1.7	≈10
V15-4	2D	2D-30°	Cyclic (pseudo-dynamic)	69	0	1.7	≈10
Vib-01	3D	3D-30°	Vibro-driven	69	≈100	0.9	≈3–4

4 Displacement and Deformation Around Pile Tips

Three model tests will be compared: V18-1, V15-4 and Vib-01 (internal names). Some relevant information concerning these tests is listed in Table 2. The test paths are illustrated schematically in Fig. 5. Note that the "time" axis is strongly stretched for the vibro-test compared to the two quasi-static tests.

A good comparability of all three tests was achieved due to the similar pile tip shape and almost equal initial soil density of $I_D = 69\,\%$. Important differences were the stress level, the water content, the penetration mode and the dimensionality of the process. The soil displacements and deformations will be compared for all three tests. A possible evolution of pore pressures in test Vib-01 is not considered in this study.

4.1 Displacement Trajectories and Deformation Paths

Figure 6a shows displacement trajectories of selected points in vicinity to the 2D-pile tip during monotonic penetration into dry sand. The axes on the left resp. bottom are the coordinates with respect to the pile symmetry plane in horizontal and the

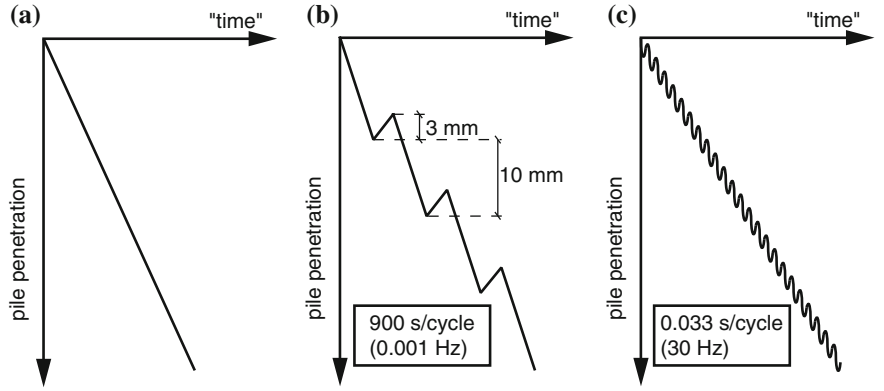

Fig. 5 Schematic test paths in **a** V18-1, **b** V15-4 and **c** Vib-01

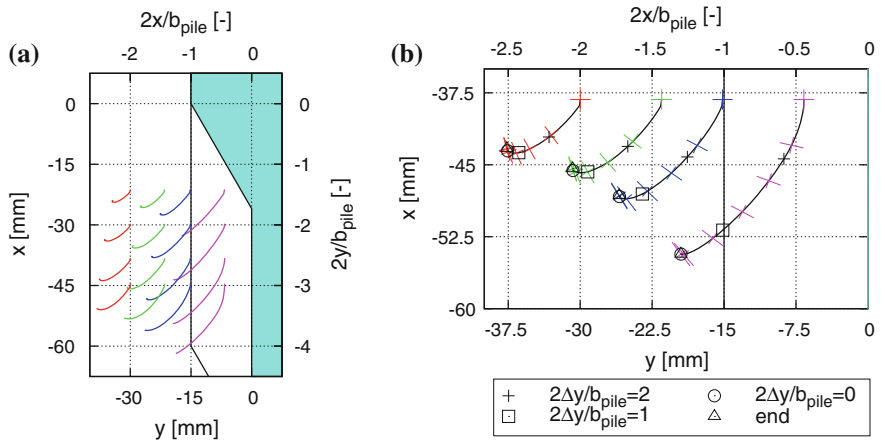

Fig. 6 Selected displacement trajectories during monotonic plane strain model pile penetration evaluated via DIC: **a** overview, **b** detailed figure with deformed elements in principal strain directions; $I_{D0} = 69\,\%$ and $S_R = 0\,\%$

pile shoulder in vertical direction, see Fig. 4. These coordinates are normalized with $b_{\text{pile}}/2$ on the top and right axis. The initial pile position is shown in blue color. The end position is indicated by solid lines. The region below the pile tip (vertical projection) corresponds to coordinates $x \in (-b_{\text{pile}}/2, b_{\text{pile}}/2)$. Displacement trajectories for sand elements in vertical columns (same initial horizontal position) are plotted in the same line color. Figure 6b is a detailed view on four soil elements in a horizontal cross section. The current normalized vertical position of the soil element with respect to the current position of the pile shoulder is indicated for four selected moments: $2\Delta y/b = 2$, $2\Delta y/b = 1$, $2\Delta y/b = 0$ and for the end of the test. $2\Delta y/b = 0$ is the moment where the soil element passes the vertical level of the pile shoulder. In addition to the trajectories, the current shape of each element is plotted as a cross in

the principal strain directions, see Fig. 4d. The cross represents the current minimal and maximal width of the element in the view plane.

Figure 6 indicates that the sand is pushed downwards and to the side as the pile tip passes the sand elements. The vertical displacement downwards is larger in the regions under the vertical projection of the pile tip. The outer sand elements have a predominant horizontal displacement component. Some sand elements show a slight uplift towards the end of the penetration process. This detail will be taken into consideration later on.

The two lower rows show very similar displacement trajectories. They can be treated as representative displacement patterns due to pile penetration. The sand regions above do not undergo the whole history of the pile penetration process. The third row (counted from the top) is therefore shown separately in a detailed view in Fig. 6b. Figure 6b also illustrates the chronology of the process and the occuring deformations. As the pile approaches vertically towards the sand elements the horizontal displacement component becomes more and more dominant. The further pile penetration causes only very small displacements. These displacements are oriented upwards for the sand elements outside of the pile projection. The displacement upwards start before the pile shoulder has passed the sand elements. For the sand elements in direct vicinity to the pile tip, the displacements are purely downwards.

The deformation mode resulting from pile penetration was often reported: Below the pile tip, the deformation regime is roughly vertical compression/horizontal extension and beside the pile tip the opposite, vertical extension/horizontal compression. A deformation pattern like this was observed in experiments (e.g. in [15]) and is also obtained qualitatively from FE analysis [1]. The direction of minimal width (maximal compression) is oriented approximately tangentially to the displacement trajectory as long as an element is under the pile projection. When the pile tip passes an element, a counter-clockwise rotation of directions of principal strains with respect to the trajectory can be seen.

Figure 7 shows the same curves for similar points during an alternating or pseudo-dynamic pile penetration in dry sand. The pile penetration consists in movements downwards interupted by phases of 3 mm pile displacement upwards, see Fig. 5. The effective penetration per "cycle" is 10 mm.

The displacement trajectories during cyclic penetration in Fig. 7a are very similar to the displacement patterns during monotonic penetration. In Fig. 7b, the cycles can be analysed more clearly. The cycles are like loops attached to the monotonic path. For small displacements upwards, a positive vertical displacement occurs due to the stress relief. Subsequently, the soil elements move to the side towards the symmetry axis. In the new penetration phase, the monotonic path is rapidly reached and followed.

In Fig. 7a, a problem related to DIC evaluation of pile penetration processes can be seen. The element in the second row and right column (highest pink trajectory) shows a strong displacement downwards as the pile tip has already passed this element. This displacement pattern is anormal and is in distinct contrast to other elements starting from the same horizontal position. It can be seen, that the considered soil element ends up close to the pile and actually overlapes the pile shaft, which is physically

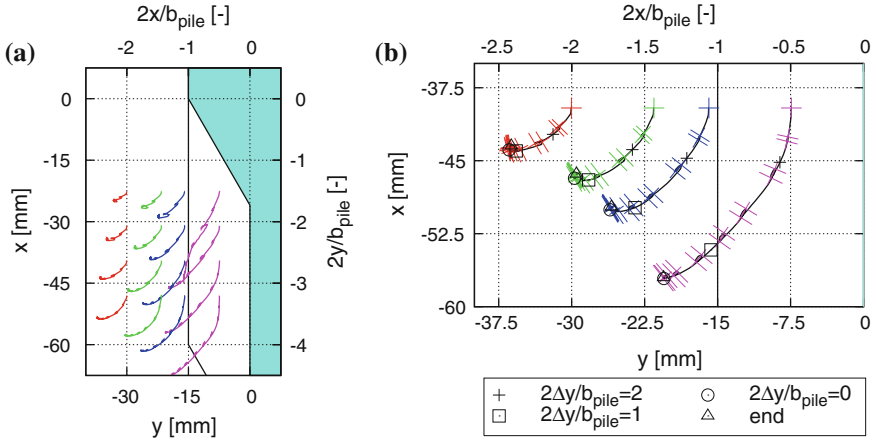

Fig. 7 Selected displacement trajectories during pseudo-dynamic plane strain model pile penetration evaluated via DIC: **a** overview, **b** detailed figure with deformed elements in principal strain directions; $I_{D0} = 69\,\%$ and $S_R = 0\,\%$

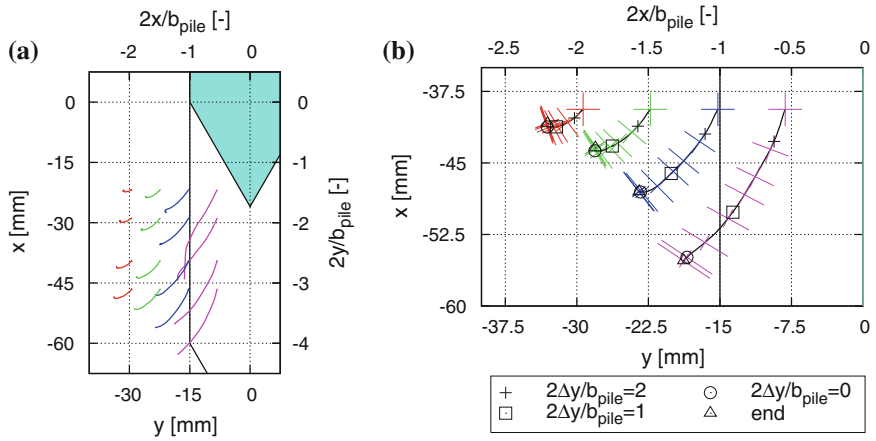

Fig. 8 Selected displacement trajectories during vibrodriven model pile penetration evaluated via DIC: **a** overview, **b** detailed figure with deformed elements in principal strain directions; $I_{D0} = 69\,\%$ and $S_R \approx 100\,\%$

not possible. This behaviour results from an erratic DIC evaluation. When a sand region is located too close to the pile tip, it may happen that parts of the test patch contain sections of the pile. These sections disturb the evaluation of displacements and the soil displacement contains erroneously portions of the pile displacement (rigid body). Thus, the evaluation of regions in vicinity to sand-structure interfaces have to be treated very carefully.

Figure 8 shows similar displacement trajectories for the vibro-driven 3D-pile penetration. Globally, the displacements are similar the quasistatic 2D-pile penetration. Quantitative comparison will be made in Fig. 9.

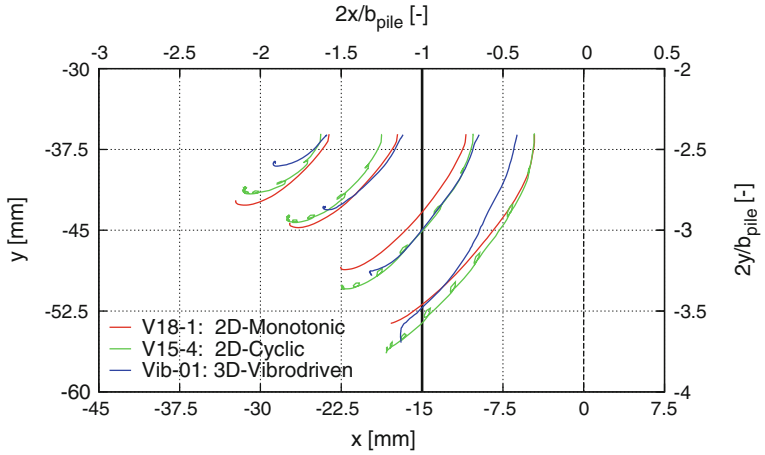

Fig. 9 Comparison of displacement trajectories for monotonic, cyclic and vibrodriven model pile penetration

One detail stands in contrast to Figs. 6 and 7: the sand elements near the pile shaft tend to move downwards along the shaft when the pile tip has already passed these elements. This calculated displacement was verified and does not result from an erratic DIC evaluation.

Figure 9 compares the displacement trajectories in the three penetration modes for selected points. Note that the positions of the selected points are slightly different because the size of the DIC patches differ. The vertical offset was eliminated in order to start from one given vertical level. The horizontal position was not altered.

Figure 9 shows a qualitatively similar displacement mechanism for all three penetration modes. The sand elements in the vertical projection of the pile are pushed down- and sidewards with a predominant vertical component. They end up next to the pile shaft as the pile has passed. The outer sand elements are moved more to the side and show a slight uplift as the penetration continues. The two plane strain tests are in very good agreement. The vertical displacements downwards of the sand elements below the pile tip is slightly stronger in the cyclic test. Comparing the 2D tests and 3D vibrodriven test, important differences can be seen. The horizontal displacements for the 3D vibrodriven case are significantly lower than in the 2D cases. This difference is more pronounced for the sand element outside of the pile projection and results at least in parts from the dimensionality of the problem. In plane strain conditions, a horizontal displacement of a sand element is not necessarily connected to a volume change. The 3D case is comparable to a rotationally symmetric process, where a horizontal displacement results in a strain in the offplane direction (circumferential). Thus, a smaller horizontal displacement of the outer sand elements is sufficient to compensate the additional penetrated pile volume and dilation effects. Figure 10 illustrates the dimensionality effects observed in the displacement trajectories.

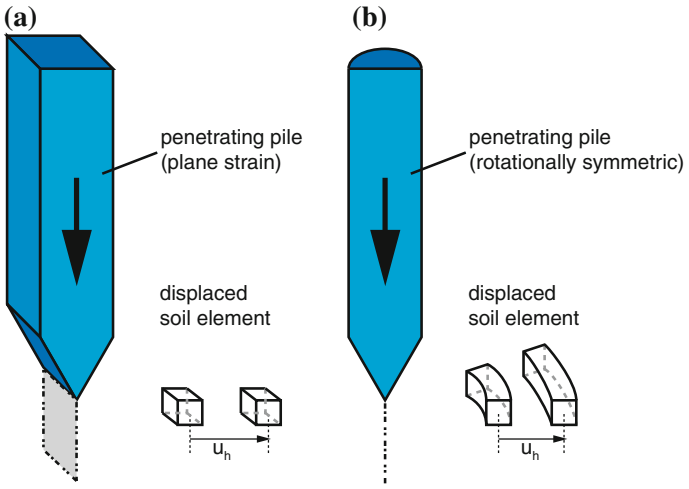

Fig. 10 Illustration of the dimensionality effect during pile penetration

Another important difference between the quasi-static and the dynamic test is the displacement of sand elements in vicinity to the pile shaft when the tip has passed. As already discussed, these sand elements show the clear tendency to follow the pile displacement downwards.

Towards the end of the outer displacement trajectories, a small but significant detail between monotonic and cyclic/vibro-driven penetration can be seen: the outer sand regions tend to move towards the pile shaft, when the pile tip is located below these elements. This important detail is discussed in the next chapter.

5 Stress Redistribution Around Pile Tips

The phenomenon of "friction fatigue" (also called the "h/R effect") is known to be a governing factor in the penetration process of a pile as well as in the evaluation of initial capacity of driven piles [7, 16]. "Friction fatigue" is defined as the decrease of shaft friction at a given depth as the pile penetrates further. It was shown to occur during cyclic and dynamic penetration. For monotonic penetration, "friction fatigue" is not to be observed [9]. "Friction fatigue" corresponds to a significant relaxation of horizontal (radial) stress in the sand regions adjacent to the pile shaft and is at least partly explained by the soil behaviour under cyclic loading. Thus, the name "friction fatigue" is not completely correct as the cause is a relief or relaxation of radial stress and the effect is a decrease of ultimate shaft friction (assuming a constant contact friction angle). Therefore we prefer to use the term "stress relaxation" in the following.

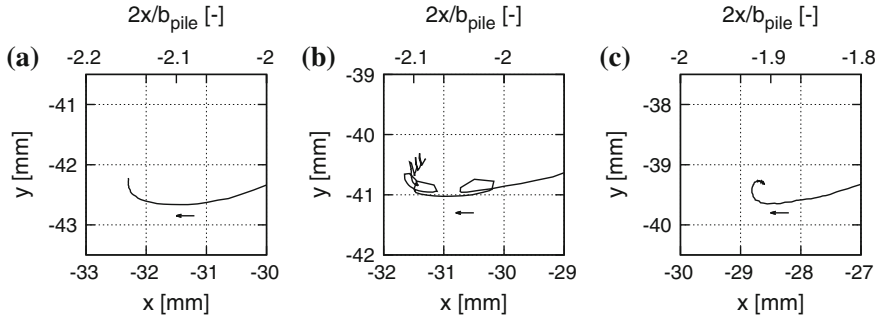

Fig. 11 End (*tail*) of displacement trajectory for **a** V18-1, **b** V15-4 and **c** Vib-01

5.1 Experimental Evidence of Stress Relaxation Along the Shaft

The investigation of relaxation effects requires the measurement of the evolution of displacements and forces resp. stresses and strains. During this study only displacements have been measured. Therefore the results can only used in an indicative manner and further investigation is needed.

The trend at the end (or tail) of displacement trajectories of elements near to the pile shaft is considered to be an indicator for the occurence of stress relaxation [16]. Figure 11a–c shows a detailed view on this section of the trajectory for the three tests. The sand elements in the third row of the first column are compared (red curves in Figs. 6, 7 and 8). The small arrows indicates the direction of displacement.

The global shape of the trajectories in Fig. 11a–c is similar: the sand is pushed sidewards and then undergoes a small uplift. However, the displacement trend towards the end contrasts sharply. During monotonic penetration (Fig. 11a) the sand element remains at a constant horizontal position. The distance between sand element and pile shaft does not change. During cyclic and vibro-driven penetration, a clear trend of displacement towards the pile shaft is observed.

6 Discussion of the Results

6.1 Comparison with Other Model Tests and FE Simulation

The presented results are in good agreement with other model tests on pile penetration. The global penetration mechanism is found similar, although different pile diameter, tip inclination and penetration modes were investigated. The observations in DIC analysis agree with the hypothesis of displacement indicators for friction fatigue and offer a plausible explanation for effects related to cyclic pile penetration.

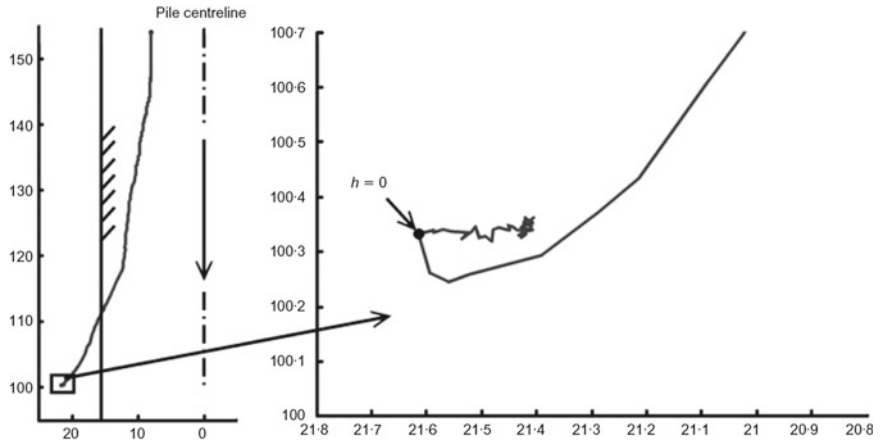

Fig. 12 Measured displacement trajectory for a sand element in direct vicinity to a penetrating model pile tip (from [15], h = Δy)

White and Bolton [15] reported similar trajectories during monotonic model pile penetration and related those to the mechanism of stress relaxation, see Fig. 12.

An explanation offers the behaviour of soils under cyclic loading conditions. Following [15], the mechanism can be described as follows: The soil direct adjacent to the pile shaft is sheared cyclically due to the cyclic motion of the pile shaft. As a consequence, it tends to contract so that the outer sand regions can move towards the pile shaft. The reaction of the sand located at the pile shaft should be a combined contraction/relaxation mode. Contraction leads to the outer displacements towards the pile shaft and relaxation leads to a degradation of shaft friction ("friction fatigue"). This interpretation is in accordance to the experimental observations in [12] on the soil behaviour adjacent to a cyclically displaced wall segment with rough surface. It was found that a jamming (opposite case of relaxation) is accompanied by a displacement trend away from the soil-wall interface. In the 3D-case, circumferential arching occurs. The circumferential horizontal stress can exceed the radial horizontal stress. It is not easy to perform measurements of this stress redistribution.

In Fig. 12, it can be seen that a displacement towards the pile tip can occur even during monotonic pile penetration. In the tests presented here, such displacement was only observed during cyclic and vibro-driven penetration. One reason could be that the performed penetration depth was not sufficient.

Although a vast number of numerical simulations of pile driving are available, comparisons with the presented test results are not easy to be drawn. Either different geometries are modelled or displacement patterns are not analysed explicitly. However, some basic analogies can be seen. Large compressive strains essentially in vertical direction and extension in horizontal direction are usually observed below the pile tip, e.g. [1]. The effect of "friction fatigue" was also observed in numerical simulations, e.g. [2]. More verification of numerical work using existing model test

data is necessary in this context. It is the aim in the research unit FOR1136 to use the presented model tests for the validation of FE simulations.

6.2 Disturbing Boundary Effects

The interaction between side walls resp. observation windows and soil was neglected until now. The displacement trajectories were interpreted as representative for the soil flow around the pile tip. However, two principal effects of interaction that actually occur have to be distinguished: the mobilization of friction in the interface side wall-soil and the deflection of the side walls due to increasing horizontal earth pressure. The parasitic impact of the observation windows is not easy to evaluate but has to be taken into account in the interpretation in a qualitative manner. The qualitative influence of both effects can be summarized as follows:

- *Friction on the side walls*
  Friction between observation window and soil inhibits soil displacements along the window and leads to off-plane shear deformation of sand elements near to the window. The soil displacements and deformations can be larger in the inner part of the soil body.
- *Deflection of the side walls*
  Deflection of the observation windows leads to strains in the off plane direction. For the 2D-case, volumetric strain can no longer be evaluated assuming plane strain conditions. This deformation cannot be evaluated with planar DIC.

The influence of frictional effects between glass and soil is considered small due to the low contact friction angle ($\approx 10°$). By observation of the free sand surface at the top, no 3D effects or arching were optically identifiable. Nevertheless, in [12] it was shown that arching effects do have an impact on the experimental results. The deflection of the side walls was measured for a monotonic test and lies in the range of 0.3 mm. Therefrom, an off-plane strain of 0.1–0.5 % can be calculated. Occuring strains during the test results presented here, reach a few % (up to more than 20 %) and are therefore predominant compared to the off-plane strain.

FE back calculation of the experiments can take account for these boundary effects if the side walls are incorporated in the model. This leads to an important improvement of comparability between test and simulation and can even enhance the interpretation of the experiment.

7 Summary and Outlook

In this contribution, the soil displacements and strains occurring during model pile penetration were investigated. Effects of penetration mode and dimensionality (plane strain-like or 3D) were studied using two test facilities: Quasi-static monotonic and

cyclic plane strain penetration was performed in a large scale interface test device and vibrodriven pile penetration was performed in a half-cylinder test device. Soil deformations were evaluated using DIC. Representative displacement trajectories of sand elements with different horizontal distances to the pile were compared. The overall penetration mechanism is similar although pile penetration mode, tip shape and degree of saturation differ. A marked dimensionality effect was demonstrated. The evaluated horizontal soil displacements were significantly larger in plane strain pile penetration than in 3D-vibro-driven penetration. Indicators for stress relaxation were shown to appear during cyclic plane strain pile penetration and during vibrodriven pile penetration. Future investigation will focus on the link between DIC evaluation of soil deformation and stress measurements on the model pile.

The tests presented include the effect of pile penetration. In subproject 6 of the research group FOR 1136, the soil liquefaction around vibrating pile tips is investigated numerically [5, 6]. However, in these simulations, the pile vibrates around a constant position, the effect of penetration is neglected. In order to compare simulations and results, future tests will be adapted to that boundary value problem. A modified pile with flat ended tip will be used for that purpose.

Acknowledgments The work presented in this paper was supported by the German Research Foundation (DFG) as part of the research project "Central project of the researchers group FOR 1136 with demonstrator experiments". The authors acknowledge the financial support.

References

1. Dijkstra, J., Broere, W., van Tol, A.: Experimental investigation into the stress and strain development around a displacement pile. In: Proceedings of the sixth European Conference on Numerical Methods in Geotechnical Engineering, pp. 595–600 (2006)
2. Grabe, J., Mahutka, K.-P.: Finite-Elemente-Analyse zur Vibrationsrammung von Pfählen. Bautechnik 82, Heft 9 (2005)
3. Klotz, U., Coop, M.R., Taylor, R.N.: Zur Verteilung von Spitzendruck, Mantelreibung und Radialspannung bei Installation von Rammpfählen in Sanden. Pfahlsymposium, pp. 201–221, Braunschweig (2001)
4. Lehane, B.M., White, D.J.: Lateral stress changes and shaft friction for model displacement piles in sand. Can. Geotech. J. **42**, 1039–1052 (2005)
5. Osinov, V.A., Chrisopoulos, St., Triantafyllidis, Th.: Numerical study of the deformation of saturated soil in the vicinity of a vibrating pile. Acta Geotechnica (2012). doi:10.1007/s11440-012-0190-7
6. Osinov, V.A., Triantafyllidis, Th.: Modelling soil liquefaction around a vibrating pile. The influence of soil permeability. 3rd Workshop "Holistic simulation of geotechnical installation processes", Karlsruhe (2014)
7. Randolph, M.F., Dolwin, J., Beck, R.: Design of driven piles in sand. Géotechnique **44**(3), 427–448 (1994)
8. Rebstock, D.: Verspannung und Entspannung von Sand entlang von Baukörpern. Diss. (2011). http://digbib.ubka.uni-karlsruhe.de/volltexte/1000023891
9. Rimoy, S.P.: Ageing and axial cyclic loading studies of displacement piles in sands. Diss, Imperial College London (2013)
10. Vennemann, P.: JPIV-software package for particle image velocimetry (2007). http://www.jpiv.vennemann-online.de

11. Vogelsang, J., Huber, G., Triantafyllidis, Th., Schindler, U.: Pfahlpenetration in nichtbindigem Boden: Großmaßstäbliche Modellversuche und Nachrechnungen. Pfahlsymposium, 409 Braunschweig (2013)
12. Vogelsang, J., Huber, G., Triantafyllidis, Th.: Demonstrator experiments on significant effects during pile installation. 2nd Workshop "Holistic simulation of geotechnical installation processes", Karlsruhe (2013)
13. Vogelsang, J., Zachert, H., Huber, G., Triantafyllidis, Th.: Effects of soil deposition on the initial stress state in model tests: experimental results and FE simulation. 3rd Workshop "Holistic simulation of geotechnical installation processes", Karlsruhe (2014)
14. Vogelsang, J., Huber, G., Triantafyllidis, Th: A large scale soil-structure interface testing device. Geotech. Test. J. **36**(5), 613–625 (2013). doi:10.1520/GTJ20120213, ISSN 0149-6115
15. White, D.J., Bolton, M.D.: Displacement and strain paths during plane-strain model pile installation in sand. Géotechnique **54**(6), 375–397 (2004)
16. White, D.J., Lehane, B.M.: Friction fatigue on displacement piles in sand. Géotechnique **54**(10), 645–658 (2004)
17. Wienbroer, H.: Umlagerung von Sand infolge Wechselbeanspruchung. Diss. Veröffentlichungen des Instituts fr Bodenmechanik und Felsmechanik (IBF) am Karlsruher Institut fr Technologie (KIT), Heft 174, Karlsruhe (2011)